

TiO_x-based self-rectifying memory device for crossbar WORM memory array applications

Li-Ping Fu(傅丽萍), Xiao-Qiang Song(宋小强), Xiao-Ping Gao(高晓平), Ze-Wei Wu(吴泽伟), Si-Kai Chen(陈思凯), and Ying-Tao Li(李颖弢)

Citation: Chin. Phys. B, 2021, 30 (**1**): 016103. DOI: 10.1088/1674-1056/abc548
Journal homepage: http://cpb.iphy.ac.cn; http://iopscience.iop.org/cpb

What follows is a list of articles you may be interested in

Extended damage range of $(Al_{0.3}Cr_{0.2}Fe_{0.2}Ni_{0.3})_3O_4$ high entropy oxide films induced by surface irradiation

Jian-Cong Zhang(张健聪), Sen Sun(孙森), Zhao-Ming Yang(杨朝明), Nan Qiu(裘南), Yuan Wang(汪渊)
Chin. Phys. B, 2020, 29 (**6**): 066104. DOI: 10.1088/1674-1056/ab8374

First-principles calculations of solute-vacancy interactions in aluminum

Sha-Sha Zhang(张莎莎), Zheng-Jun Yao(姚正军), Xiang-Shan Kong(孔祥山), Liang Chen(陈良), Jing-Yu Qin(秦敬玉)
Chin. Phys. B, 2020, 29 (**6**): 066103. DOI: 10.1088/1674-1056/ab8458

First principles study of interactions of oxygen-carbon-vacancy in bcc Fe

Yuan You(由园), Mu-Fu Yan(闫牧夫), Ji-Hong Yan(闫纪红), Gang Sun(孙刚), Chao Wang(王超)
Chin. Phys. B, 2019, 28 (**10**): 106102. DOI: 10.1088/1674-1056/ab3a8f

Self-compliance multilevel storage characteristic in HfO_2-based device

Xiao-Ping Gao(高晓平), Li-Ping Fu(傅丽萍), Chuan-Bing Chen(陈传兵), Peng Yuan(袁鹏), Ying-Tao Li(李颖弢)
Chin. Phys. B, 2016, 25 (**10**): 106102. DOI: 10.1088/1674-1056/25/10/106102

Localized deep levels in $Al_xGa_{1-x}N$ epitaxial films with various Al compositions

Shi Li-Yang, Shen Bo, Yan Jian-Chang, Wang Jun-Xi, Wang Ping
Chin. Phys. B, 2014, 23 (**11**): 116102. DOI: 10.1088/1674-1056/23/11/116102

TiO_x-based self-rectifying memory device for crossbar WORM memory array applications*

Li-Ping Fu(傅丽萍)[1,2], Xiao-Qiang Song(宋小强)[1,2], Xiao-Ping Gao(高晓平)[3,†], Ze-Wei Wu(吴泽伟)[2], Si-Kai Chen(陈思凯)[2], and Ying-Tao Li(李颖弢)[1,2,‡]

[1] *Key Laboratory of Special Function Materials and Structure Design, Ministry of Education, Lanzhou University, Lanzhou* 730000, *China*
[2] *School of Physical Science and Technology, Lanzhou University, Lanzhou* 730000, *China*
[3] *Key Laboratory of Sensor and Sensing Technology, Gansu Province, Lanzhou* 730000, *China*

(Received 2 October 2020; revised manuscript received 26 October 2020; accepted manuscript online 28 October 2020)

Resistive switching with a self-rectifying feature is one of the most effective solutions to overcome the crosstalk issue in a crossbar array. In this paper, a memory device based on Pt/TiO_x/W structure with self-rectifying property is demonstrated for write-once-read-many-times (WORM) memory application. After programming, the devices exhibit excellent uniformity and keep in the low resistance state (LRS) permanently with a rectification ratio as high as 10^4 at ± 1 V. The self-rectifying resistive switching behavior can be attributed to the Ohmic contact at TiO_x/W interface and the Schottky contact at Pt/TiO_x interface. The results in this paper demonstrate the potential application of TiO_x-based WORM memory device in crossbar arrays.

Keywords: resistive switching memory, write-once-read-many-times (WORM), self-rectifying, crossbar array

PACS: 61.72.jd, 68.60.–p, 72.20.–I, 73.40.Rw **DOI:** 10.1088/1674-1056/abc548

1. Introduction

Resistive switching (RS) memory device has been considered to be one of the most promising candidates for next-generation nonvolatile memories due to its simple structure, high switching speed, excellent scalability, low power consumption, high integration density, and compatibility with the current complementary metal oxide semiconductor (CMOS) technology.[1–5] As one type of RS memory device, write-once-read-many-times (WORM) memory devices are receiving increasing interest because they are widely used in all kinds of permanent data storage applications such as archival storage equipment, secure databases, as well as electronic labels.[6–8] To achieve high storage capacity, crossbar array with the smallest cell size of $4F^2$ is adopted. Generally, the integration of an addition selection diode to each cell is used to suppress the unexpected sneak current in crossbar structure.[8,9] Recently, the WORM memory devices with self-rectifying characteristics in low resistance state (LRS) provide a more desirable solution to suppress the sneak current without the externally added diode. However, the rectification ratios of most of the reported WORM memory devices with self-rectifying characteristics are not very high.[10,11] In previous work, a self-rectifying WORM memory device based on n^+-Si/ZrO_2/Pt structure with a high rectification ratio over 10^4 was demonstrated,[12] in which highly doped crystal silicon was used as the bottom electrode. However, from three-dimensional (3D) high-density integration point of view, crystal silicon is not expected.[13]

In this paper, by using tungsten (W) as the bottom electrode, we demonstrate a high-performance self-rectifying WORM memory device with a simple Pt/TiO_x/W structure. After programming the fresh device to LRS by applying the voltage of -5 V, a high rectification ratio as high as 10^4 is obtained. Such a high rectification ratio can overcome the crosstalk issue in crossbar array without extra diodes. In addition, the physical mechanism is investigated.

2. Experiments

The titanium oxide-based WORM memory devices in this study were prepared using the following processes. A 70-nm-thick W bottom electrode (BE) was deposited on SiO_2/Si substrate by sputtering. Subsequently, 20-nm-thick titanium oxide film was deposited on the W bottom electrode by atomic layer deposition (ALD) system. $TiCl_4$ was used as the Ti precursor and H_2O was used as the oxygen precursor. An atomic layer deposition cycle with 4 steps was adopted for this experiment. The 4 steps were $TiCl_4$ reactant, N_2 purge, H_2O reactant, and N_2 purge, respectively. During the deposition, the temperature was maintained at 150 °C. Finally, 70-nm-thick square-shaped platinum (Pt) top electrodes (TE) with areas of 100×100 μm^2 were deposited and defined by photolithography and lift-off process to form Pt/TiO_x/W structure devices. The composi-

*Project supported by the National Natural Science Foundation of China (Grant Nos. 61774079 and 61664001), the Science and Technology Plan of Gansu Province, China (Grant No. 20JR5RA307), and the Key Research and Development Program of Gansu Province, China (Grant No. 18YF1GA088).

†Corresponding author. E-mail: xp.gao@gsas.ac.cn
‡Corresponding author. E-mail: li_yt06@lzu.edu.cn

© 2021 Chinese Physical Society and IOP Publishing Ltd

tion and binding energy analysis of the deposited TiO_x film was performed using x-ray photoelectron spectroscope (XPS). The current–voltage (I–V) characteristics of the fabricated devices were measured by a Keithley 4200-SCS semiconductor characterization system at room temperature. During the measurements, the bias voltage was applied on the top electrode while the bottom electrode was grounded.

3. Results and discussion

To confirm the chemical nature and the existence of the defects in the deposited TiO_x film, the XPS depth profiling was performed as shown in Fig. 1. From XPS depth profiling, the TiO_x film is composed of two layers (here referred to as top layer and bulk layer). The XPS spectrum of the top layer film (surface to 4 nm) in Fig. 1(a) shows that O 1s peak is associated with TiO_2 layer indicating the stoichiometric oxide layer. In contrast, the XPS spectrum of the bulk layer film (4 nm to 20 nm) in Fig. 1(b) shows that the profile of the O 1s spectrum can be fitted by two Gaussian components at 531.0 eV and 531.9 eV. The component of the low binding energy locating at 531.0 eV is associated with the O^{2-} ions from the Ti-O bonding, and the high binding energy locating at 531.9 eV is related to oxygen deficiencies of the TiO_x layer,[14,15] which indicates metal excess nonstoichiometric TiO_x layer of the bulk layer film.

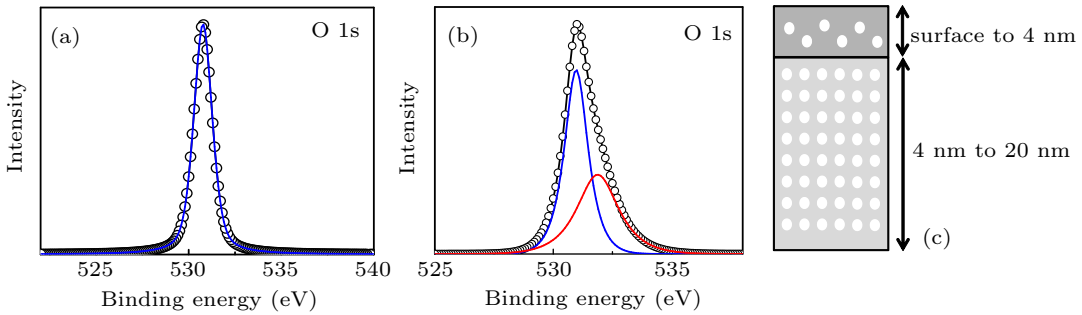


Fig. 1. XPS spectra of O 1s in the deposited TiO_x film. (a) Top layer film: from surface to 4 nm in depth, and (b) bulk layer film: from 4 nm to 20 nm. (c) Schematic representation of the structure of the deposited TiO_x film in depth.

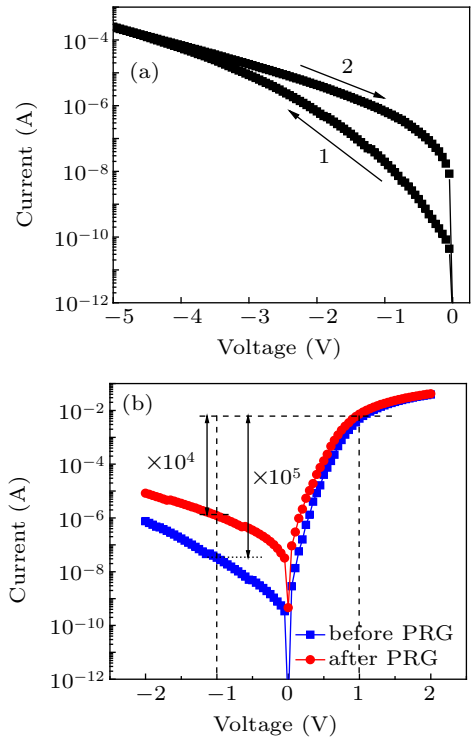


Fig. 2. (a) Programming process (PRG) of the as-deposited fresh device. (b) Typical I–V curves of the Pt/TiO_x/W memory device before and after PRG.

Figure 2 shows the typical I–V curves of the Pt/TiO_x/W structure device. As shown in Fig. 2(a), the as-deposited fresh device is in an initial high resistance state (HRS). By sweeping the voltage from zero to a negative voltage, a gradual increase of the device current can be observed, and the device switches from the initial HRS to low resistance state (LRS) by increasing the voltage to about −5 V and then keeps in LRS permanently and steadily. Figure 2(b) shows the typical I–V curves of the Pt/TiO_x/W device before and after the programming process (PRG). It can be observed that the resistance ratio between HRS and LRS exceeds 10 by using a −1 V readout voltage. More importantly, a pronounced rectifying characteristic with the rectification ratio as high as 10^4 can be obtained after PRG. With such a self-rectifying behavior in LRS, the undesired sneak current can be suppressed, and the crosstalk issue can be avoided effectively in the crossbar array.

Although various models have been proposed to explain the resistive switching behaviors in WORM memory devices, the intrinsic mechanism is still unclear, especially for the self-rectifying WORM memory device.[10–12] Based on the XPS data shown in Figs. 1(a) and 1(b), the fabricated TiO_x film is composed of two layers, including top stoichiometric TiO_2 layer with high resistance and nonstoichiometric TiO_x bulk layer with more oxygen deficiencies, as schematically summarized in Fig. 1(c). Compared with the top TiO_2 layer, the bulk TiO_x layer shows much higher conductivity due to the existence of more oxygen deficiencies. Therefore, when a negative voltage is applied to activate the fresh memory de-

vice, the high voltage is only applied on the top high resistance layer and it causes soft-breakdown of the top high resistance layer,[16] leading to the LRS of the Pt/TiO$_x$/W WORM memory device after the programming process. To further clarify the self-rectifying current conduction mechanism of the Pt/TiO$_x$/W WORM memory device, the I–V curves in both HRS and LRS are analyzed using different theoretical models. As shown in Fig. 3, ln$I$ has a linear relation to $V^{1/2}$ for both HRS and LRS, indicating that the resistive switching behavior of the Pt/TiO$_x$/W WORM memory device is dominated by the Shcottky emission model.[8,12] In our previous work, it has been confirmed that the TiO$_x$/W interface is Ohmic contact and the Pt/TiO$_x$ interface is Shcottky contact.[17] Therefore, the electron injecting barrier at the Pt/TiO$_x$ interface is higher than that at the TiO$_x$/W interface, resulting in the self-rectifying resistive switching behavior in the Pt/TiO$_x$/W WORM memory device.

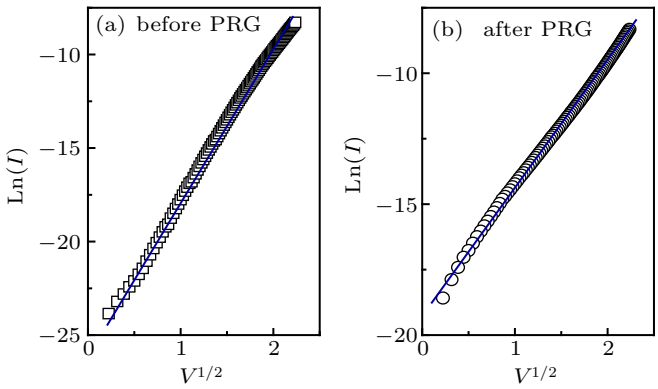


Fig. 3. Analysis of the ln$I$–$V^{1/2}$ curves (a) before and (b) after PRG with the Shcottky emission model.

To evaluate the uniformity of the Pt/TiO$_x$/W WORM memory device, the statistical measurements of resistances distribution of 20 randomly chosen devices in different positions of the two inches wafer were performed. Figure 4(a) shows the statistical data of the resistances obtained by ±1 V read voltages before (R_B) and after (R_A) programming. And the mean values (μ) and standard deviations (σ) of R_B and R_A at −1 V and 1 V read voltages are 1.09×10^8 Ω (9.63×10^7 Ω), 424 Ω (64 Ω), 2.35×10^6 Ω (8.28×10^5 Ω), and 244 Ω (34 Ω), respectively. Except for the R_B at −1 V read voltage, all the other resistances exhibit narrow distributions with good uniformity. Furthermore, it can be seen from Fig. 4 that the reading window margin at the −1 V read voltage excesses 10, which is large enough to distinguish these two states to store information. Furthermore, the HRS rectifying ratio higher than 10^5 and LRS rectifying ratio as high as 10^4 can be observed for different memory devices. The retention characteristic of the Pt/TiO$_x$/W WORM memory device is also characterized and shown in Fig. 4(b). First, the retention test is carried out on the fresh device before PRG. Then, the same device is programmed to the LRS by applied a −5 V voltage. The resistances in both states are stable and no significant degradation is observed for over 10^4 s, which demonstrate the nonvolatile storage capability of the Pt/TiO$_x$/W WORM memory device.

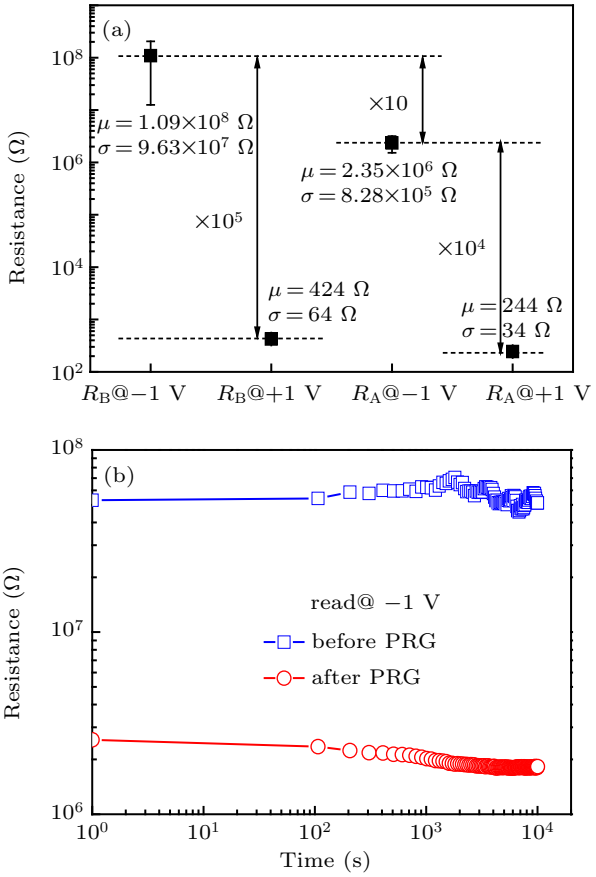


Fig. 4. Device-to-device distributions of the resistances obtained by ±1 V read voltages before and after PRG. All the statistical data are obtained from 20 random devices. (b) Retention characteristic of the Pt/TiO$_x$/W WORM memory device.

4. Conclusions

We have successfully demonstrated a self-rectifying WORM memory device with promising memory characteristics such as excellent uniformity and good retention. Moreover, a remarkable self-rectifying effect in LRS could be also observed in the device, which can minimize the crosstalk issue in the crossbar array. The Ohmic contact at TiO$_x$/W interface and the Schottky contact at Pt/TiO$_x$ interface are suggested to explain the self-rectifying behavior of the Pt/TiO$_x$/W WORM memory device.

References

[1] Zhao X L, Ma J, Xiao X H, Liu Q, Shao L, Chen D, Liu S, Niu J B, Zhang X M, Wang Y, Cao R R, Wang W, Di Z F, Lv H B, Long S B and Liu M 2018 *Adv. Mater.* **30** 1705193
[2] Li Y T, Long S B, Lv H B, L Q, Wang Q, Wang Y, Zhang S, Lian W T, Liu S and Liu M 2011 *Chin. Phys. B* **20** 017305
[3] Li C, Belkin D, Li Y, Yan P, Hu M, Ge N, Jiang H, Montgomery E, Lin P, Wang Z, Strachan J P, Barnell M, Wu Q, Williams R S, Yang J J and Xia Q 2018 *Nat. Commun.* **9** 2385

[4] Li Y T, Long S B, Lv H B, Liu Q, Wang W, Wang Q, Huo Z L, Wang Y, Zhang S, Liu S and Liu M 2011 *IEEE Electron Device Lett.* **32** 363
[5] Liu Q, Sun J, Lv H B, Long S B, Yin K B, Wan N, Li Y T, Sun L T and Liu M 2012 *Adv. Mater.* **24** 1844
[6] M?ller S, Perlov C, Jackson W, Taussig C and Forrest S R 2003 *Nature* **426** 166
[7] Li B X, Yin H, Xia F, Sun B, Zhang S Y, Xia Y D, Chen Y H and Huang W 2020 *Adv. Electron. Mater.* **6** 2000109
[8] Teo E Y H, Zhang C, Lim S L, Kang E T, Chan D S H and Zhu C 2009 *IEEE Electron Device Lett.* **30** 487
[9] Ahn S E, Kang B S, Kim K H, Lee M J, Lee C B, Stefanovich G, Kim C J and Park Y 2009 *IEEE Electron Device Lett.* **30** 550
[10] Ouyang J, Chu C W, Sieves D and Yang Y 2005 *Appl. Phys. Lett.* **86** 123507
[11] Tan Y P, Song Y, Teo E Y H, Ling Q D, Lim S L, Lo Patrick G, Chan D S H and Kang E T and Zhu C X 2008 *J. Electrochem. Soc.* **155** H17
[12] Zuo Q Y, Long S B, Yang S Q, Liu Q, Shao L B, Wang Q, Zhang S, Li Y T, Wang Y and Liu M 2010 *IEEE Electron Device Lett.* **31** 344
[13] Lv H B, Li Y T, Liu Q, Long S B, Li L and Liu M 2013 *IEEE Electron Device Lett.* **34** 229
[14] Kuznetsov M V, Zhuravlev J F and Gubanov V A 1992 *J. Electron. Spectrosc.* **58** 169
[15] Hsu C C, Wang S Y, Lin Y S and Chen Y T 2019 *J. Alloy. Compd.* **779** 609
[16] Lee D S, Choi H J, Sim H J, Choi D H, Hwang H S, Lee M J, Seo S A andYoo I K 2005 *IEEE Electron Device Lett.* **26** 719
[17] Li Y T, Gong Q C and Jiang X Y 2014 *Appl. Phys. Lett.* **104** 132105